Article no. 44

THE CIVIL ENGINEERING JOURNAL 4-2019

INFLUENCE OF PANEL ZONE SIZES ON ULTIMATE BEARING CAPACITY OF H-SHAPED STEEL FRAMES

Yan Zhang, Huijuan Liu, Yuhong Yang, Enhe Bao

College of Civil Engineering and Architecture, Guilin University of Technology, Guilin 541004, China; 864476103@qq.com

ABSTRACT

In order to explore the influence of panel zone sizes on the ultimate bearing capacity of H-shaped steel frames, this study examines a steel frame structure with cross-shaped sections consisting of beams, columns and panel zones based on mechanical equilibrium principles. The area ratio of either side of the flange to the web is taken as the main parameter.

The results show that the ultimate bearing capacity ratio curves can be grouped into three types. For the first type, the plastic hinge is formed in the panel zone. For the second type, when R_{pcb}, the strong column factor, is greater than 1.2, the plastic hinge is formed at the beam end; otherwise the plastic hinge is formed in the panel zone. For the third type, when $R_{pcb} \leq 0.8$, the plastic hinge is formed in the panel zone; otherwise the plastic hinge is formed at the beam end. The ultimate bearing capacity ratio curves of the local section of H-shaped steel largely fall in the first curve type, and the ultimate bearing capacity is larger when the panel zone size is excluded from the calculation than otherwise with the former being one to five times as large as the latter.

KEYWORDS

H-shaped steel frame, Panel zone, Strong column factor, Ultimate bearing capacity

INTRODUCTION

According to the current Chinese seismic code, panel zones are usually excluded from the calculation of the bearing capacity of steel frames. Generally, a panel zone is considered as either a "strong panel zone" or "rigid panel zone" in the overall steel framework structure calculation. Studies [1, 2] show that, according to the results from the common local cyclic loading test, the panel zone yields early and features better performance in terms of elastic-plastic deformation and energy dissipation. A new conformation form to connect the H-beam with the box-shaped panel zone of the I-beam weak axis is proposed in research [3] and, according to the results of the Finite Element Analysis, the panel zone of the box-shaped joint of the I-beam weak axis is discovered to be a "strong panel zone" whose mechanical property is superior to the traditional box-section columns structure. In the research of [4], numerical results have revealed that designs according to AISC360 and Eurocode 3 resulted in significant amounts of yielding of the panel zone while the designs according to FEMA 355D resulted in minimal amount of yielding. The panel zone deformation demands were quantified and an equation used to estimate the deformation levels. Weak panel zones are designed for the two specimens to drive plastic deformation in the panel zones, the plastic deformation will mainly develop in the panel zones without apparent plastic straining at the beam ends [5]. Studies [6-8] examine rectangular columns filled with concrete and the hysteresis loop model of the panel zone of H-shaped beams. Meanwhile, the experiments also focus on the mechanical properties of rectangular steel columns with outer ring stiffeners and irregular joint zones of H-shaped steel

beams. Moreover, with the assumption of the “rigid panel zone”, the damage mechanism of the whole steel frame structure has been explored. For example, Ref. [9] has studied the dynamic response of multi-levelled steel frame structure when the maximum speed of seismic waves is 0.5m/s, however, the factor of column base should be almost equal to strong column factor but more than 1.5; Ref. [10, 11] study American steel frame structure using the model of the sheared mass and the flexure bar system to comprehensively evaluate the anti-seismic effect while columns beams and column bases are articulated in the frame; Ref. [12] examines the elasto-plasticity dynamic performance of a super high-rise structure. Previous studies are mainly focused on the elastic-plastic performance of different plane zones in steel frames and the elastic-plastic performance of high-rise steel structures. Consequently, little light has been shed on the effect of the sizes of panel zones on the ultimate bearing capacity of H-shaped steel frames, especially of Chinese-manufactured H-shaped steel.

To unveil general patterns regarding the ultimate bearing capacity of Chinese H-shaped steel frames, this study examines cruciform steel frames consisting of beams, columns and panel zones for analysis purposes. Also, based on the principles of equilibrium mechanics, this study takes into account the flange-to-web area ratio as the main parameter while also considering other factors such as the axial compression ratio of columns, the span-depth ratio of structures, the depth-to-width ratio of panel zones and the ratio of panel zone width to floor height.

Research model

Panel zones are commonly designed strong enough to avoid premature buckling due to the shear load transferred by the adjacent beams. This design concept has been accepted by most of the countries, such as the US and China [13]. As shown in Figure 1(a), exemplifying a regular H-shaped steel frame where its storey height equals span, a cruciform steel frame consisting of common beams columns and panel zones is taken for analysis purposes. The size of the analytical model is also shown in Figure 1(a). In this model, the connections of beams, columns and panel zones are rigid, but supports are hinged. The calculation diagram with external force is shown in Figure 1 (b).

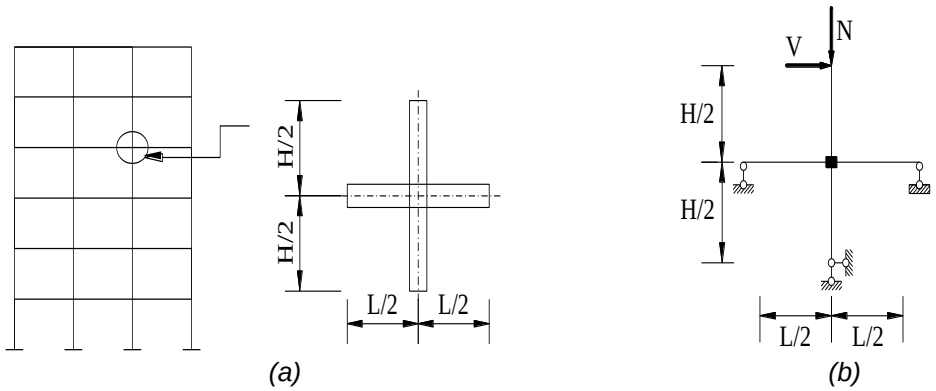

Fig. 1 - Local cruciform steel frame model

When the axial compression ratio (μ) is taken into consideration, Equation 1 is used to calculate the plastic section modulus in the direction of the major axis, and Equation 2 is used to calculate the plastic section modulus of the H-shaped steel beam [14].

$$W_{pc} = \begin{cases} \frac{\beta(4+\beta_c)-\mu^2(2+\beta_c)^2}{4\beta_c(2+\beta_c)} Ah & (\mu < \frac{A_w}{A}) \\ \frac{1}{2}Ah(1-\mu) & (\mu \geq \frac{A_w}{A}) \end{cases} \quad (1)$$

$$W_{pb} = Ah(\frac{4\beta_b+1}{8\beta_b+4}) \quad (2)$$

In the equations, β is the area ratio of either side of the flange (A_f) to the web (A_w) (the flange-to-web area ratios of beam and column are β_b and β_c, respectively); h is the section height of the H-shaped steel; A is the section area of the component.

Model analysis

Stress analysis

When the horizontal load (V) and the axial load (N) are applied to the local steel frame model, as shown in Figure 1(b), the pattern of force distribution in the beam, the column and the panel zone is shown in Figure 2(a). The bending moments in steel moment resisting frames are transferred between the beams and columns in the frame through either rigid or semi-rigid connections or joints [15]. The moment distribution in the column, the beam-end and the center node are shown in Figure 2(b).

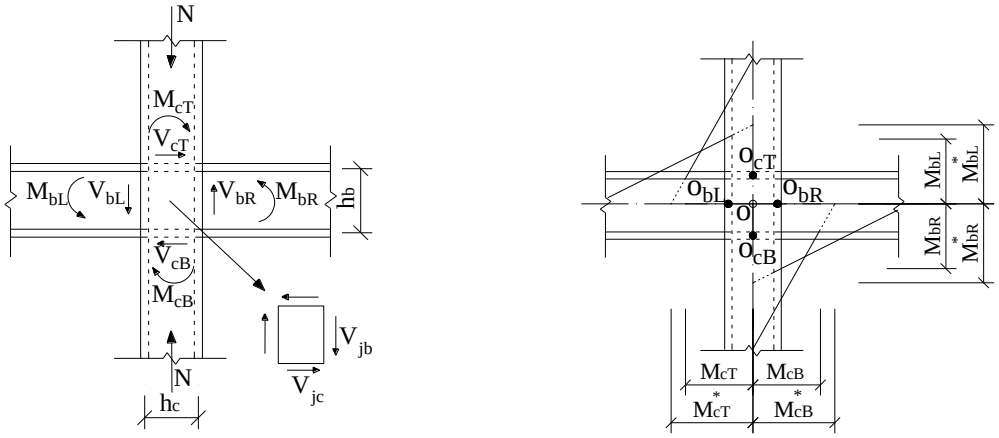

(a) Force distribution in beam, column and panel *(b) Moment distribution in column, beam-end and node center*

Fig. 2 - Stress analysis of the model

In this model, h_b and h_c stand for the heights of the flange center in the beam and the column, respectively and the same calculation method is used both for the panel zone and for the column. So according to Figure 2(a), the equilibrium equations of the force in the panel zone are listed as follows:

$$M_j = V_{jb}h_c = V_{jc}h_b \quad (3)$$

$$V_{jc} = \frac{M_{bL}+M_{bR}}{h_b} - \frac{V_{cT}+V_{cB}}{2} \quad (4)$$

$$V_{jb} = \frac{M_{cT}+M_{cB}}{h_c} - \frac{V_{bL}+V_{bR}}{2} \quad (5)$$

where $M_{cT} = M_{cB} = 0.5V(H - h_b)$, $V_{cT} = V_{cB} = V$, $M_{bL} = M_{bR} = 0.5VH(L - h_c)/L$ and $V_{bL} = V_{bR} = VH/L$.

M_j is the bending moments of panel zone; M_{bL} and M_{bR} are the bending moments at both beam ends; V_{bL} and V_{bR} are the shear forces at both beam ends. M_{cT} and M_{cB} are the bending moments at both the upper end and the lower end of the column; V_{cT} and V_{cB} are the shear forces of the beam; V_{jc} and V_{jb} are the shear forces of the panel zone for column and beam.

According to Figure 2(b), the bending moment equations of the beam, the column and the center node are shown below:

$$M_{bL}^* + M_{bR}^* = M_{cT}^* + M_{cB}^* = M_j^* \quad (6)$$

$$M_{bL}^* + M_{bL}^* = M_{pbL} + M_{pbR} + (V_{bL} + V_{bR}) \times h_c/2 \quad (7)$$

$$M_{cT}^* + M_{cB}^* = M_{pcT} + M_{pcB} + (V_{cT} + V_{cB}) \times h_b/2 \quad (8)$$

$$M_j^* = M_j + (V_{cT} + V_{cB}) \times h_b/2 + (V_{bL} + V_{bR}) \times h_c/2 \quad (9)$$

Assuming that the whole section plastic moments at column ends, beam ends and in the panel zone are M_{pc} (the top and bottom end moments of the column consequently being M_{pcT} and M_{pcB}), M_{pb} (the left and right end moments of the beam being M_{pbL} and M_{pbR}) and M_{pj}, respectively, then correspondingly, the moments of the column, beam and panel zone in the node center O are M^*_{pcT}, M^*_{pcB}, M^*_{pbL}, M^*_{pbR} and M^*_{pj}, respectively. The equations concerning these variables are:

$$M_{pbL}^* + M_{pbR}^* = M_{pbL} + M_{pbR} + (V_{bL} + V_{bR}) \times h_c/2 \quad (10)$$

$$M_{pcT}^* + M_{pcB}^* = M_{pcT} + M_{pcB} + (V_{cT} + V_{cB}) \times h_b/2 \quad (11)$$

$$M_{pj}^* = M_{pj} + (V_{cT} + V_{cB}) \times h_b/2 + (V_{bL} + V_{bL}) \times h_c/2 \quad (12)$$

where, when the whole section plastic moment is reached, the following equations are true:

$$V_{cT} = V_{cB} = 2M_{pc}/(L - h_b) \quad (13)$$

$$V_{bL} = V_{bR} = 2M_{pb}/(L - h_c) \quad (14)$$

$$V_{cT} = V_{cB} = M_{pj}^*/H \quad (15)$$

$$V_{bL} = V_{bR} = M_{pj}^*/L \quad (16)$$

When Equation 13 – 16 are substituted into 10 – 12, the following equations can be obtained:

$$M_{pcT}^* = M_{pcB}^* = M_{pc}^* = M_{pc}/(1 - h_b/H \quad (17)$$

$$M_{pbL}^* = M_{pbR}^* = M_{pb}^* = M_{pb}/(1 - h_c/L \quad (18)$$

$$M_{pj}^* = M_{pj}/(1 - (h_c/L + h_b/H)) \quad (19)$$

Also the two equations below are taken into account :

$$M_{pc} = W_{pc} \times f_y \quad (20)$$

$$M_{pb} = W_{pb} \times f_y \tag{21}$$

The equation of the plastic moment in the whole section of the H-shaped steel column panel zone is written as [16]:

$$M_{pj} = (Ah_b\sqrt{1-u^2}) \times f_v/\sqrt{3}(2\beta_c + 1) \tag{22}$$

When the panel zone size is taken into consideration, V_u^{j*} the ultimate horizontal bearing capacity of the cross-shaped steel frame section, is expressed as:

$$V_u^{j^*} = Min\{2M_{pc}^*, 2M_{pb}^*, M_{pj}^*\} \times \frac{1}{H} \tag{23}$$

Accordingly, when the panel zone size is excluded, V_u^j, the ultimate horizontal bearing capacity of the cross-shaped steel frame section, is expressed as:

$$V_u^j = Min\{2M_{pc}, 2M_{pb}\} \times \frac{1}{H} \tag{24}$$

And the strong column factor is calculated as:

$$R_{pcb} = M_{pc}/M_{pb} \tag{25}$$

Influence of panel zone size on ultimate bearing capacity of H-shaped steel analysis model

Based on Equation 23 and 24, β is taken as the main parameter under study (given the fact that there is no significant difference in the β values of a certain section with the same specification, an average β value is assigned to each specific section. Therefore, β_b in narrow flange beam of Chinese-made H-shaped steel is 0.7, in middle flange beam is 1.06, and β_c in wide flange column of Chinese-made H-shaped steel is 1.49). Additionally, μ, L/H (span-to-depth ratio of structure), h_b/h_c (depth-to-width ratio of panel zone) and h_c/H (ratio of panel zone width to floor height) are taken into consideration as well for the study to examine the difference between the results from when the panel zone size is included in and excluded from the model. In both cases, the panel zone which is defined as the portion of the column contained within the beam-to-column joint can be subjected to high shear stresses arising from the unbalanced moments at interior joints that are produced by lateral loads such as wind and earthquake forces [17].

In Figure 3, the vertical axis shows the ultimate bearing capacity ratio (V_u^{j*}/V_u^j), while the horizontal axial indicates strong column factor (R_{pcb}).

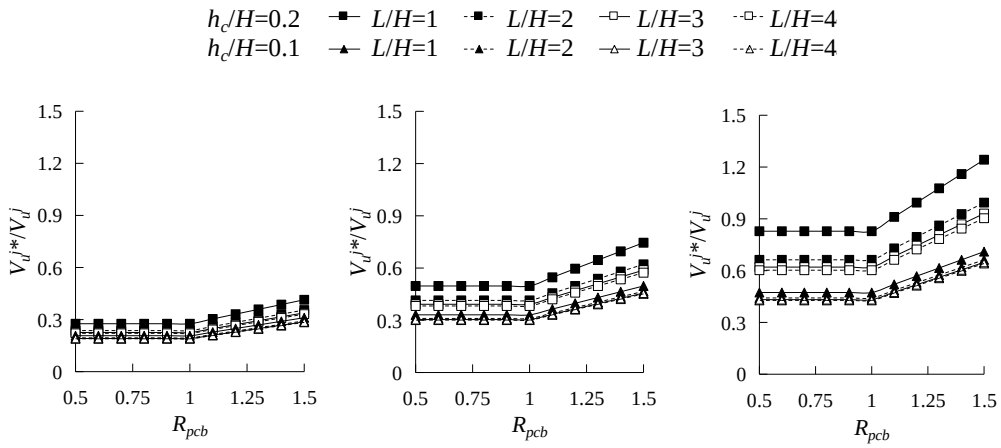

(a) Axial compression ratio of column μ=0

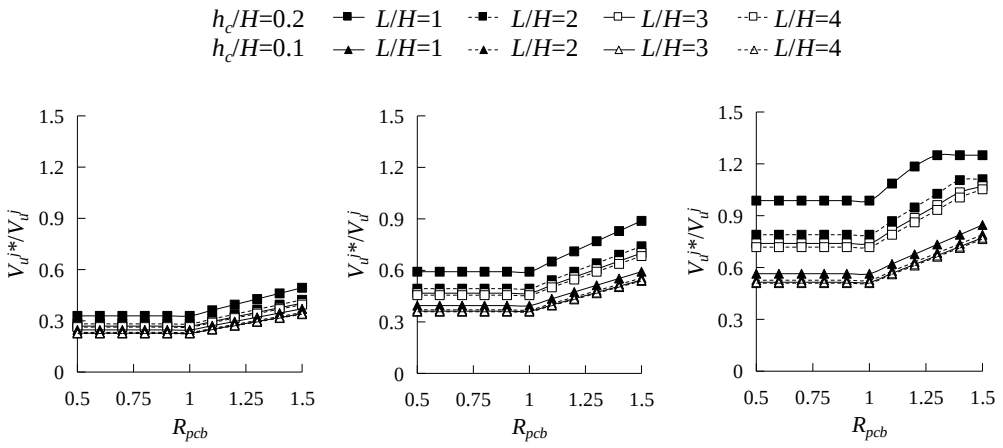

(b) Axial compression ratio of column μ=0.3

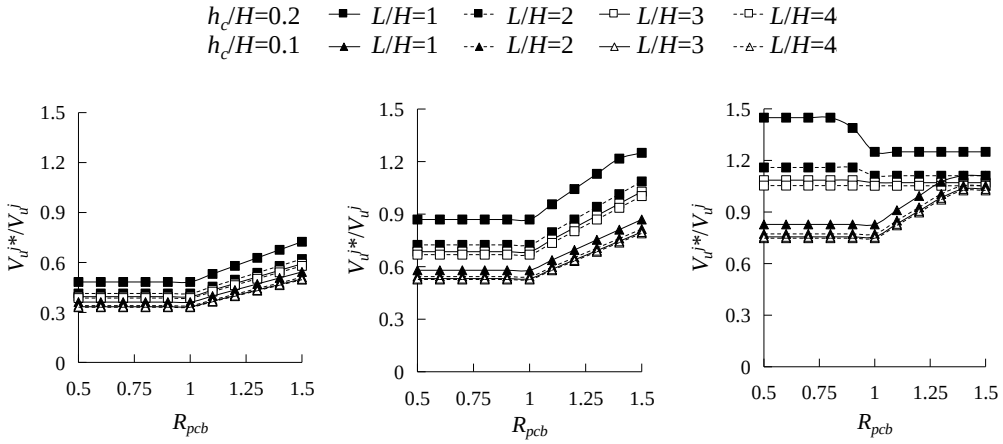

(c) Axial compression ratio of column μ=0.6

Fig. 3 - Narrow flange beam of H-shaped steel (β_b=0.70)

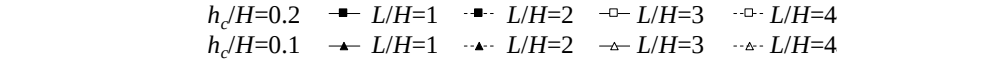

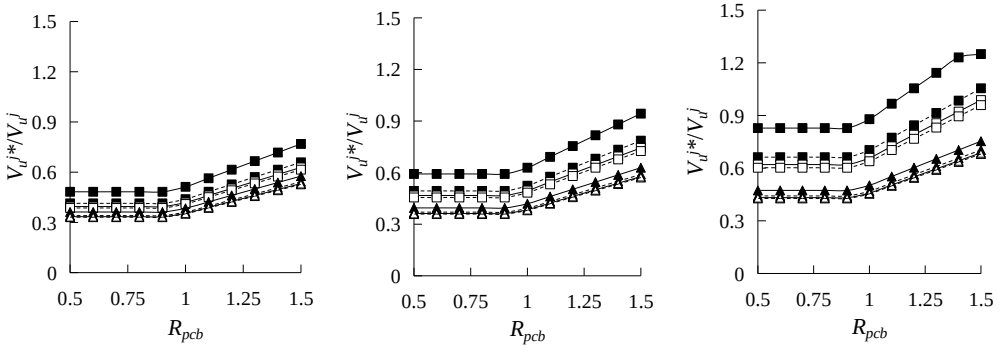

Fig. 4 - Ultimate bearing capacity ratio patterns of middle flange beam analysis model

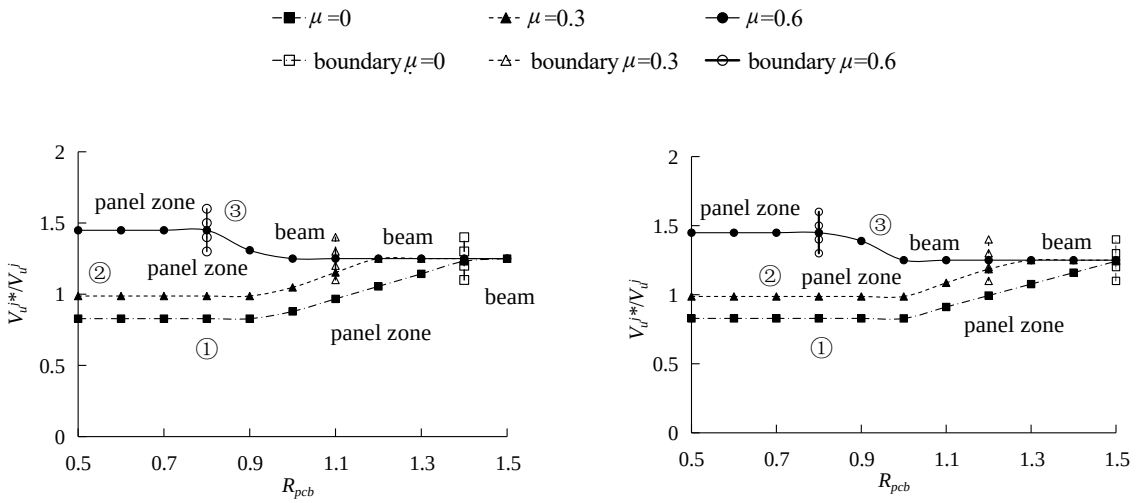

(a) Narrow flange beam of H-shaped steel (β_b =0.70) (b) Middle flange beam of H-shaped steel (β_b =1.06)

Fig. 5 - Plastic damage change boundary of analysis model

As shown in Figure 3(a) and Figure 3(b), when the panel zone size is not taken into consideration, the ultimate bearing capacity is dependent either on the column end moment (when R_{pcb}<1) or on the beam end moment (when R_{pcb}≥1). On the other hand, when the panel zone size is taken into consideration, there are three types of curves regarding the ultimate bearing capacity. For the first type, when R_{pcb}≤1, the curve stays a horizontal line; when R_{pcb}>1, the curve turns into an oblique line going upwards as R_{pcb} increases indicating plastic damage in the panel zone, as is shown in Figure 5(a) ①. For the second type, when R_{pcb}≤1, the curve stays a horizontal line indicating plastic damage in the panel zone; when R_{pcb}>1, the curve first becomes an oblique line going upwards as R_{pcb} increases also indicating plastic damage in the panel zone, and then (as R_{pcb} grows larger) turns into a horizontal line indicating plastic damage at the beam end (see Figure 5(a) ②). For the third type, when R_{pcb}≤0.8, the curve stays a horizontal line with a relatively large vertical value indicating plastic damage in the panel zone; when R_{pcb}>0.8, the curve first becomes an oblique line going downwards as R_{pcb} increases, and then turns into a horizontal line as R_{pcb} grows larger indicating plastic damage at the beam end (see Figure 5(a) ③).

Figure 3 illustrates the $V_u^{j*}/V_u^j \sim R_{pcb}$ correlation of the narrow flange beam of H-shaped steel. In the case where μ=0, the curve where h_c/H=0.2, L/H=1 and h_b/h_c=2 grows over 1 (i.e., V_u^{j*}/V_u^j>1) when R_{pcb}>1.1; the ultimate bearing capacity is larger when the panel zone size is incorporated than otherwise. In any other cases, V_u^{j*}/V_u^j<1, specifically ranging from 0.2 to 1.0 (i.e., V_u^{j*} is one to five times of V_u^j); the ultimate bearing capacity is larger when the panel zone size is excluded. It can thus be concluded that when μ=0, V_u^j is most likely to be larger than V_u^{j*} with V_u^j being five times as large as V_u^{j*} in the most extreme case scenario. In addition, the shape of the V_u^{j*}/V_u^j - R_{pcb} curve shows great resemblance with that of Figure 5(a) ① when μ=0, and yielding all occurs in the panel zone when the panel zone size is taken into consideration.

In the case where μ=0.3, the curve where h_c/H=0.2 and h_b/h_c=2 largely grows over 1 (i.e., V_u^{j*}/V_u^j>1) when R_{pcb}>1.2; the ultimate bearing capacity is larger when the panel zone size is incorporated than otherwise. The shape of the curve shows great resemblance with that of Figure 5(a) ②. When the panel zone size is taken into consideration, yielding occurs in the panel zone (in the case where R_{pcb}<1.2) or in the beam (in the case where R_{pcb}≥1.2). In any other cases, V_u^{j*}/V_u^j<1, specifically ranging from 0.2 to 1.0 (i.e., V_u^{j*} is one to five times of V_u^j); the ultimate bearing capacity is larger when the panel zone size is excluded. It can be concluded that when μ=0.3, V_u^j is most likely to be larger than V_u^{j*} with V_u^j being five times as large as V_u^{j*} in the most extreme case scenario. In addition, the shapes of all the V_u^{j*}/V_u^j - R_{pcb} curves (except the one where h_c/H=0.2 and h_b/h_c=2) show great resemblance with that of Figure 5(a) ① when μ=0.3, and yielding all occurs in the panel zone when the panel zone size is taken into consideration.

In the case where μ=0.6, V_u^{j*}/V_u^j>1 always stands true for the curves where h_c/H=0.2 and h_b/h_c=2, and mostly stands true, when R_{pcb}>1.2, for the curves either where h_c/H=0.2 and h_b/h_c=1.5 or where h_c/H=0.1 and h_b/h_c=2; the ultimate bearing capacity is larger when the panel zone size is incorporated than otherwise. In any other cases, V_u^{j*}/V_u^j<1, specifically ranging from 0.3 to 1.0 (i.e., V_u^{j*} is one to three times of V_u^j); the ultimate bearing capacity is larger when the panel zone size is excluded. The shape of the V_u^{j*}/V_u^j - R_{pcb} curve where h_c/H=0.2 and h_b/h_c=2 shows great resemblance with that of Figure 5(a) ③. When the panel zone size is taken into consideration, yielding occurs in the panel zone (in the case where R_{pcb}≤0.8) or in the beam (in the case where R_{pcb}>0.8). The shapes of the V_u^{j*}/V_u^j - R_{pcb} curves either where h_c/H=0.2 and h_b/h_c=1.5 or where h_c/H=0.1 and h_b/h_c=2 show great resemblance with that of Figure 5(a) ②. When the panel zone size is taken into consideration, yielding occurs in the panel zone (in the case where R_{pcb}≤1.2) or in the beam (in the case where R_{pcb}>1.2). In any other cases, the shape of the V_u^{j*}/V_u^j - R_{pcb} curves shows great resemblance with that of Figure 5(a) ①. When the panel zone size is taken into consideration, yielding all occurs in the panel zone.

Figure 4 illustrates the $V_u^{j*}/V_u^j \sim R_{pcb}$ relationship of the middle flange beam analysis model (h_b/h_c=1.5, μ=0, 0.3 and 0.6). In the case where μ=0.6, the curve where h_c/H=0.2 largely grows over 1 (i.e., V_u^{j*}/V_u^j>1) when R_{pcb}>1.1; the ultimate bearing capacity is larger when the panel zone size is incorporated than otherwise. The curve has the same shape as Figure 5(a) ② does. When the panel zone size is taken into consideration, yielding occurs in the panel zone (in the case where R_{pcb}<1.2) or in the beam (in the case where R_{pcb}≥1.2). In any other cases, V_u^{j*}/V_u^j<1, specifically ranging from 0.3 to 1.0 (i.e., V_u^{j*} is one to three times of V_u^j) and showing a curve shape similar to Figure 5(a) ①; the ultimate bearing capacity is larger when the panel zone size is excluded; and yielding all occurs in the panel zone when the panel zone size is taken into consideration. According to the model analysis, the ultimate bearing capacity ratio of the middle flange beam of H-shaped steel is larger than that of the narrow flange beam.

Figure 5(a) illustrates the three curves with the largest ultimate bearing capacity ratios, each chosen from each of the three types of curves in Figure 3 (regarding narrow flange beam of H-shaped steel). Figure 5(b), in contrast, shows the ultimate bearing capacity ratio curves of middle flange beam of H-shaped steel. As is shown in Figure 5(b), in the case where μ=0, the shape of the

curve matches not the first but the second type of curve in Figure 5(a), and yielding occurs in the beam when R_{pcb}=1.5.

As is shown in Figure 3 to Figure 5, when and only when h_b/h_c=2.0, μ=0.6 and h_c/H=0.2, the shape of the ultimate bearing capacity ratio curve matches that of the third curve type, and yielding occurs in the panel zone (in the case where R_{pcb}<0.8) or in the beam (in the case where R_{pcb}≥0.8); the ultimate bearing capacity is larger when the panel zone size is incorporated than otherwise. When h_b/h_c=2.0, μ=0.3 and h_c/H=0.2 or when h_b/h_c=2.0, μ=0.6 and h_c/H=0.1, the shape of the ultimate bearing capacity ratio curve matches that of the second curve type; yielding occurs in the panel zone when R_{pcb}<1.2 or in the beam if R_{pcb}≥1.2. When yielding occurs in the beam, the ultimate bearing capacity is larger with the panel zone size incorporated than otherwise. In any other cases, the shape of the ultimate bearing capacity ratio curve matches that of the first curve type. The shape of the ultimate bearing capacity ratio curve of the local section of H-shaped steel largely matches that of the first type of curve, and a plastic hinge forms in the panel zone of the analysis model. The ultimate bearing capacity is smaller when the panel zone size is incorporated than otherwise with V_u^j being one to five times as large as V_u^{j*}. The behaviour of the panel zone plays a significant role in determining the overall stiffness and capacity of the frame [18]. Therefore, if the panel zone size is not incorporated in the calculation, the ultimate bearing capacity of an H-shaped steel frame may be overestimated, leading to unsafe structure design.

CONCLUSION

In order to examine the influence of the panel zone size on the ultimate bearing capacity of Chinese H-shaped steel frames, β, the area ratio of either side of the flange (A_f) to the web (A_w), is taken as the main research parameter and the study is based on mechanical equilibrium principles with findings shown below:

(a) The ultimate bearing capacity ratio curves can be grouped into three types. For the first type, the plastic hinge is formed in the panel zone. For the second type, when R_{pcb}, the strong column factor, is greater than 1.2, the plastic hinge is formed at the beam end, otherwise the plastic hinge is formed in the panel zone. For the third type, when R_{pcb}≤0.8, the plastic hinge is formed in the panel zone, otherwise the plastic hinge is formed at the beam end.

(b) When the height-to-width ratio of the panel zone (h_b/h_c) equals 2.0, the axial compression ratio (μ) equals 0.6 and h_c/H=0.2, the shape of the ultimate bearing capacity ratio curve matches that of the third type of curve, and the ultimate bearing capacity is larger when the panel zone size is incorporated than otherwise. In the case where h_b/h_c=2.0, μ=0.3 and h_c/H=0.2, or where h_b/h_c=2.0, μ=0.6 and h_c/H=0.1, the shape of the ultimate bearing capacity ratio curve matches that of the second type of curve. In the case where R_{pcb}≥1.2, the ultimate bearing capacity is larger when the panel zone size is incorporated than otherwise. In any other conditions, the shape of the ultimate bearing capacity ratio matches that of the first curve type.

(c) The ultimate bearing capacity ratio curves of the local section of H-shaped steel largely fall in the first curve type, which means that the plastic hinge is formed in the panel zone. The ultimate bearing capacity is smaller when the panel zone size is incorporated than otherwise with V_u^j being one to five times as large as V_u^{j*}. Therefore, if the panel zone size is not incorporated in the calculation, the ultimate bearing capacity of an H-shaped steel frame may be overestimated, leading to unsafe structure design.

(d) In the case where the panel zone size is not taken into account, the ultimate bearing capacity is dependent on the moment of the column end when R_{pcb}≤1, or on the moment of the beam end when R_{pcb}>1.

REFERENCES

[1] Pan L.L., Chen Y.Y., 2012. Experimental study on H-shaped beam-to-column connections with vertical Stiffener. Journal of Building Structures, 33(12): 1-9. DOI: 10.14006/j.jzjgxb.2012.12.004

[2] Pan L.L., Chen Y.Y., Jiao W.F., Chuan G.H., 2015. Experimental study on panel zone in spatial H-shaped beam-column connections under cyclic loading. Journal of Building Structures, 36(10): 11-19.

[3] Lu L.F., Xu Y.L., Zhou T.H., Zheng H., 2016. Experimental research on box strengthened Joint connection for weak axis of I-section column-H-shaped beam under Monotonic Loading. Journal of Building Structures, 37(2): 73-80. DOI: 10.14006/j.jzjgxb.2016.02.010

[4] Mehmet T., Cem T., 2015. Panel zone deformation demands in steel moment resisting frames. Journal of Constructional Steel Research, 110:65–75. DOI: 10.1016/j.jcsr.2015.02.017

[5] Chen Y.Y., Pan L.L., Jia L.J., 2017. Post-buckling ductile fracture analysis of panel zones in welded steel beam-to-column connections. Journal of Constructional Steel Research, 132: 117-129. DOI: 10.1016/j.jcsr.2017.01.015

[6] Toshiyuki F., 2007. Local elasto-plastic behavior of steel beam to concrete-filled square steel tube column moment connections—Simple model of load-deformation relations for connection details using internal diaphragms or internal diaphragms with extended flanges. Journal of Structural and Construction Engineering, 617: 177-184.

[7] Toshiyuki F., 2015. Local elasto-plastic behavior of steel beam to concrete-filled square steel tube column moment connections—Model of load-deformation relations for eccentric details using internal diaphragms or internal diaphragms with extended flanges. Journal of Structural and Construction Engineering, 714(80): 1337-1345.

[8] Shintaro M., Takuro O., Ryusuke I., Tsuyoshi T., 2013. Elasto-plastic behavior of offset beam-to-column connection panels with exterior diaphragms. Journal of Structural and Construction Engineering, 692(10):1823-1830. DOI: 10.3130/aijs.78.1823

[9] Iathong C., Yuji K., Keiichiro S., 2015. Effects of input direction of ground motion and column overdesign factor on seismic response of 3D steel moment frames with square tube columns. Journal of Structural and Construction Engineering, 717(80): 1773-1783.

[10] Hiroyuki T., Gregory M., Laura L., 2007. Evaluation of seismic response of multi-story structures using dynamic stability coefficients. Journal of Structural and Construction Engineering, 618(8): 65-72.

[11] Hiroyuki T., Gregory M., Laura L., 2010. Continuous Column Effects of Gravity Columns in U.S. Steel Moment-resisting Frame Structures—Continuous columns effects in steel moment frames in perspective of dynamic stability Part 2. Journal of Structural and Construction Engineering, 650(75): 761-770.

[12] Zhang H.D., Wang Y.F., 2012. Energy-based study on the dynamic elastic plasticity seismic capacity of a high-rise steel structure. China Civil Engineering Journal, 45(6): 65-73. DOI: 10.15951/j.tmgcxb.2012.06.015

[13] AISC (American Institute of Steel Construction), 2016. AISC 314-16: Specification for Structural Steel Buildings. AISC, Chicago, Illinois, USA.

[14] BRI (Building Research Institution of Japan), 2006. Design specifications of steel structure joint 3: 206. BRI, Tokyo, Japan.

[15] Trahair N.S., Bradford M.A., Nethercot D.A., 2001. The behaviour and design of steel structures to BS5950. 3rd British ed. Spon press, London, UK. 356-390.

[16] Inoue K., 2003. The theory and design of the building steel structure. The Kyoto University Publishing House, Kyoto, Japan.

[17] Heidarpour A., Bradford M.A., 2009. Elastic behaviour of panel zone in steel moment resisting frames at elevated temperatures. Journal of Constructional Steel Research, 65(2): 489-496. DOI: 10.1016/j.jcsr.2008.02.010

[18] Castro J.M., Elghazouli A.Y., Izzuddin B.A., 2005. Modelling of the panel zone in steel and composite moment frames. Engineering Structures, 27(1): 129-144. DOI: 10.1016/j.engstruct.2004.09.008